

Correlating Mössbauer and Solution- and Solid-State ^{117}Sn NMR Data with X-ray Diffraction Structural Data of Triorganotin 2-[(*E*)-2-(2-Hydroxy-5-methylphenyl)-1-diazenyl]benzoates

Rudolph Willem,^{*,†,‡} Ingrid Verbruggen,[†] Marcel Gielen,[‡] Monique Biesemans,^{†,‡} Bernard Mahieu,[§] Tushar S. Basu Baul,^{||} and Edward R. T. Tiekink^{*,⊥}

High-Resolution NMR Centre (HNMR) and Department of General and Organic Chemistry of the Faculty of Applied Sciences (AOSC), Free University of Brussels (VUB), Pleinlaan 2, B-1050 Brussel, Belgium, INAN, Catholic University of Louvain, Chemin du Cyclotron 2, B-1348 Louvain-la-Neuve, Belgium, Department of Chemistry, The University of Adelaide, Australia 5005, and North Eastern Hill University, Regional Sophisticated Instrumentation Centre, Chemical Laboratory, Shillong 793003, India

Received June 18, 1998

A series of $\text{R}_3\text{SnO}_2\text{CR}'$ compounds, where R = Me (**1**), Et (**2**), ⁿBu (**3**), Ph (**4**), and cHex (**5**) and $\text{R}'\text{CO}_2$ is the carboxylate residue of 2-[(*E*)-2-(2-hydroxy-5-methylphenyl)-1-diazenyl]benzoic acid, has been shown by multinuclear magnetic resonance studies to be monomeric in solution. Crystallography shows that monomeric four-coordinate species are found in the solid state for **4** and **5** but polymeric structures with five-coordinate tin atoms are found for **1–3**. The different behavior is ascribed to the steric demands of the tin-bound substituents. A fair correlation is found between the difference in ^{117}Sn chemical shift between the solution and solid states and the carbonyl oxygen–tin distance of the compounds **1–5**, only when the data of **4**, R = Ph, are omitted. This indicates that the mesomeric effect of the phenyl group does not express its influence to the same extent in the solid and solution states, unlike the inductive effects. By contrast, a good correlation including **4** is found between the Mössbauer quadrupole splitting and the difference in ^{117}Sn chemical shift between the solution and solid states. This shows that the nature of the organic group on the tin atom contributes to similar extents to the values of the ^{117}Sn chemical shifts in solution and solid state, independently of the existence or not of mesomeric effects, and that the parallel behavior of QS and ^{117}Sn chemical shifts is geometry independent.

Introduction

The structural chemistry of triorganotin carboxylates, $\text{R}_3\text{Sn}(\text{O}_2\text{CR}')$, continues to receive attention owing to their industrial and agricultural/biocidal applications.¹ More recently, certain derivatives have displayed potential as anticancer agents.² The first structure determination of $\text{R}_3\text{Sn}(\text{O}_2\text{CR}')$, employing single-crystal X-ray diffraction methods, was reported in 1968,³ and since then over 60 crystal structures have been reported, underpinning the importance of these compounds.⁴ In the solid state, four basic motifs have been observed for $\text{R}_3\text{Sn}(\text{O}_2\text{CR}')$ when it is assumed that possible additional

coordination to tin originates only from the carboxylate oxygen atoms; other motifs arise when other potential donor atoms reside in the organic residue (R').⁴ Essentially discrete, monomeric entities featuring four-coordinate, distorted tetrahedral tin atom geometries (**Ia**) or discrete, five-coordinate distorted cis-trigonal bipyramidal geometries (**Ib**) represent one of the two common motifs; the difference between (**Ia**) and (**Ib**) rests in the magnitude of the $\text{Sn}-\text{O}_{\text{carbonyl}}$ interaction (for structures, see Chart 1). The second common motif is polymeric, owing to the presence of bidentate bridging carboxylate ligands and displays five-coordinate distorted trans-trigonal bipyramidal geometries (**II**). The remaining motifs **III** and **IV** have, thus far, been reported only for $[\text{Bu}_3\text{Sn}(\text{O}_2\text{CC}_6\text{H}_3\text{F}_2-2,6)]^5$ and $[\text{Ph}_3\text{Sn}(\text{O}_2\text{CR}'')] \text{ where } \text{O}_2\text{CR}'' \text{ is } N\text{-phthaloylglycinate.}^6$ Motif **III** is cyclotetrameric with bidentate bridging carboxylate ligands and distorted trans-trigonal bipyramidal geometries as found for **II**; motif **IV** is similar but cyclohexameric. A consistent rationale for the adoption

[†] HNMR, Free University of Brussels.

[‡] AOSC, Free University of Brussels.

[§] Catholic University of Louvain.

^{||} North Eastern Hill University.

[⊥] The University of Adelaide.

(1) (a) Davies, A. G.; Smith, P. J. In *Comprehensive Organometallic Chemistry*; Wilkinson, G., Stone, F. G. A., Abel, E. W., Eds.; Pergamon Press: Oxford, 1982; Vol. 2. (b) Blunden, S. J.; Chapman, A. H. In *Organometallic Compounds in the Environment*; Craig, P. J., Ed.; Longman Group: Harlow, London, 1986. (c) Champ, M. A.; Seligman, P. F. In *Organotin: Environmental Fate and Effects*; Champ, M. A., Seligman, P. F., Eds.; Chapman & Hall: London, 1996; Chapter 1.

(2) Gielen, M. *Coord. Chem. Rev.* **1996**, *151*, 41.

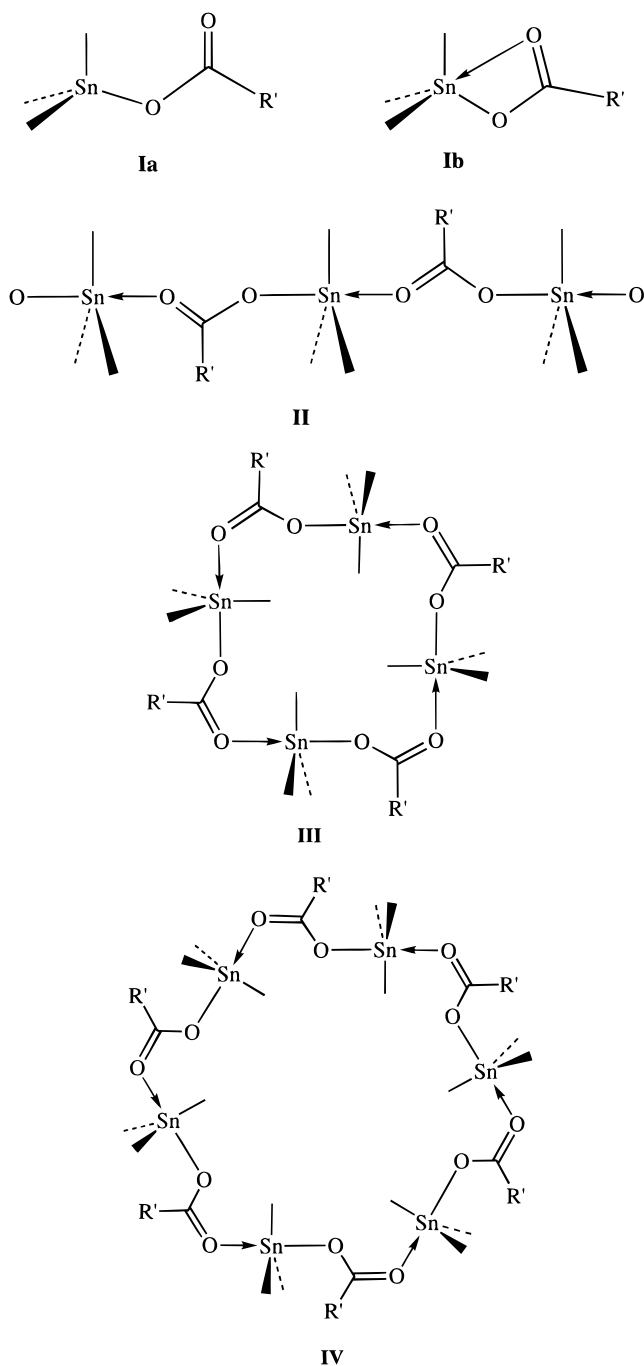
(3) Alcock, N. W.; Timms, R. E. *J. Chem. Soc. A* **1968**, 1873, 1876.

(4) Tiekink, E. R. T. *Trends Organomet. Chem.* **1994**, *1*, 71; *Appl. Organomet. Chem.* **1991**, *5*, 1.

(5) Gielen, M.; El Khouloufi, A.; Biesemans, M.; Kayser, F.; Willem, R.; Mahieu, B.; Maes, D.; Lisgarten, J. N.; Wyns, L.; Moreira, A.; Chattopadhyay, T. K.; Palmer, R. A. *Organometallics* **1994**, *13*, 2849.

(6) Ng, S. W.; Kumar Das, V. G.; Pelizzi, G.; Vitali, F. *Heteroatom. Chem.* **1990**, *1*, 433.

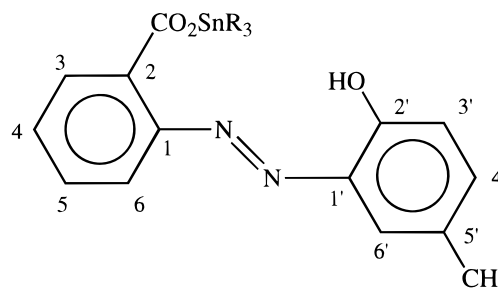
Chart 1



of different motifs for $R_3Sn(O_2CR')$ systems has yet to be delineated and is the focus of the work reported herein.

Factors that may contribute to the remarkable structural diversity include electronic properties and steric factors of the triorganotin center and/or carboxylate ligand and, less tangibly, crystal packing effects. It has been stated that there is a clear preference for the polymer structure of type (II), except in case of excessive bulk, either at the tin-bound organic group or at the carboxylate moiety, in which case type I is favored.⁷ While it is generally true that bulky organic groups at tin preclude the adoption of the polymeric motif, the

difficulty in evoking steric arguments alone is found in the following pairs of structures. Thus, for $[R_3Sn(O_2CC_4H_3S)]$ motif II is found for $R = Me$ ⁸ and motif I for $R = Ph$,⁹ i.e., consistent with steric arguments. However, when the carboxylate ligand is acetate, both $R = Me$ ¹⁰ and $R = Ph$ ¹¹ adopt motif II. A systematic study of the structural chemistry of $R_3Sn(O_2CR')$, where either R or R' is varied, depends on the availability of suitable crystals, a goal that has generally proved elusive, with a few notable exceptions but where the emphasis has been on an examination of systematically varying R' .¹² In the course of studies in this area, a series of $R_3Sn(O_2CR')$ compounds has provided X-ray quality crystals in which R has been varied and R' held constant, i.e., where $R = Me, Et, ^nBu, Ph$,¹³ and $cHex$ and $R'CO_2$ is the carboxylate moiety derived from 2-[(*E*)-2-(2-hydroxy-5-methylphenyl)-1-diazenyl]benzoic acid.



The purpose of the present report is 2-fold. The first focus aims at comparing systematically the structure of these compounds in the solid state, as assessed by X-ray diffraction, and in the solution state, as assessed by solution NMR data. In particular, it is analyzed to which extent varying the organic substituent on the tin atom modulates the solid-state geometry of the triorganotin carboxylate around the tin atom. The second focus, given that X-ray diffraction structures are available, is to investigate to what extent solid-state spectroscopic parameters arising from Mössbauer spectroscopy as well as from ^{117}Sn CP MAS NMR may serve as reliable indicators of the solid-state structure, whenever X-ray data is unavailable.

Experimental Section

Materials and Synthesis. The $R = Me, Et, ^nBu$, and $cHex$ compounds were prepared from the equimolar reaction of sodium [*o*-(2-hydroxy-5-methylphenylazo)benzoate] and R_3SnCl (Br in the case of $R = Et$) in methanol solution under reflux for 2 h. The solid obtained after the removal of the solvent was washed with petroleum ether (40–60 °C), and the residue was extracted with chloroform, filtered, and dried over anhydrous sodium sulfate. Slow evaporation of the filtrate afforded

(8) Sandhu, G. K.; Verma, S. P.; Tiekink, E. R. T. *J. Organomet. Chem.* **1990**, *393*, 195.

(9) Ng, S. W.; Kumar Das, V. G.; van Meurs, F.; Schagen, J. D.; Straver, L. H. *Acta Crystallogr.* **1989**, *C45*, 568.

(10) Chih, H.; Penfold, B. R. *J. Cryst. Mol. Struct.* **1973**, *3*, 285. Smyth, D. R.; Tiekink, E. R. T. *Z. Kristallogr.* **1998**, *213*, 605.

(11) Molloy, K. C.; Purcell, T. G.; Quill, K.; Nowell, I. W. *J. Organomet. Chem.* **1984**, *267*, 237.

(12) (a) Swisher, R. G.; Vollano, J. F.; Chandrasekhar, V.; Day, R. O.; Holmes, R. R. *Inorg. Chem.* **1984**, *23*, 3147. (b) Holmes, R. R.; Day, R. O.; Chandrasekhar, V.; Vollano, J. F.; Holmes, J. M. *Inorg. Chem.* **1986**, *25*, 2490.

(13) (a) Basu Baul, T. S.; Tiekink, E. R. T. *Z. Kristallogr.* **1996**, *211*, 489. (b) Harrison, P. G.; Lambert, K.; King, T. J.; Majee, B. *J. Chem. Soc., Dalton Trans.* **1983**, 363.

(7) Molloy, K. C.; Quill, K.; Nowell, I. W. *J. Chem. Soc., Dalton Trans.* **1987**, 101.

Table 1. Crystallographic Data for $R_3Sn(O_2CR')$

	R = Me	R = Et	R = ⁿ Bu	R = cHex
formula	C ₁₇ H ₂₀ N ₂ O ₃ Sn	C ₂₀ H ₂₆ N ₂ O ₃ Sn	C ₂₆ H ₃₈ N ₂ O ₃ Sn	C ₃₂ H ₄₄ N ₂ O ₃ Sn
fw	419.1	461.1	545.3	623.4
cryst dimens (mm)	0.18 × 0.19 × 0.46	0.05 × 0.27 × 0.29	0.04 × 0.17 × 0.37	0.11 × 0.27 × 0.50
cryst syst	monoclinic	orthorhombic	monoclinic	triclinic
space group	<i>P</i> 2 ₁ / <i>c</i>	<i>Pbca</i>	<i>P</i> 2 ₁ / <i>n</i>	<i>P</i> $\bar{1}$
<i>a</i> (Å)	13.908(2)	16.935(6)	11.162(9)	10.348(2)
<i>b</i> (Å)	9.775(1)	24.099(9)	10.068(1)	16.516(3)
<i>c</i> (Å)	13.424(3)	10.398(7)	25.270(5)	9.953(1)
α (deg)				91.18(1)
β (deg)	100.84(1)		102.52(3)	117.70(1)
γ (deg)				87.59(2)
<i>V</i> (Å ³)	1792.4(5)	4243(2)	2772(2)	1504.7(4)
<i>Z</i>	4	8	4	2
<i>D</i> _{calcd} (g cm ⁻³)	1.553	1.443	1.306	1.376
μ (cm ⁻¹)	14.40	12.24	9.48	8.83
θ range (deg)	3.0–27.5	3.0–25.0	3.0–27.5	3.0–27.5
no. of reflns measd	4568	4215	7122	7342
no. of unique reflns	4393	4215	6785	6955
no. of reflns used ^a	2756	1427	3750	4432
no. of variables	208	235	277	343
<i>R</i>	0.034	0.071	0.044	0.044
<i>R</i> _w	0.040	0.074	0.052	0.043
residual e ⁻ /Å ³	0.45	0.85	0.48	0.62

^a $I \geq 3.0\sigma(I)$.

the desired product. For the R = Ph compound, a different procedure was employed. This was prepared by refluxing the acid form of the ligand with (Ph₃Sn)₂O (2:1) in anhydrous benzene. The water formed during the reaction was removed azeotropically using a Dean–Stark apparatus. The compound was isolated by following the work up procedure as described above.

Crystals of the R = Me, Et, ⁿBu, cHex, and Ph (isolated as an acetone hemi-solvate^{13a}) compounds were obtained from the slow evaporation of an acetone/benzene (1:4), acetone/benzene (3:1), petroleum ether (40–60 °C), benzene, and acetone/methanol (1:9) solutions of the compounds, respectively.

Physical Data. For R = Me: red blocks, yield 63%, mp 171–172 °C. Anal. Found: C, 48.8; H, 4.7; N, 6.7. Calcd for C₁₇H₂₀N₂O₃Sn: C, 48.7; H, 4.8; N, 6.7. For R = Et: orange plates, yield 90%, mp 108–109 °C. Anal. Found: C, 52.1; H, 5.5; N, 6.1. Calcd for C₂₀H₂₆N₂O₃Sn: C, 52.1; H, 5.7; N, 6.1. For R = ⁿBu: orange blocks, yield 80%, mp 59–60 °C. Anal. Found: C, 57.2; H, 6.7; N, 5.1. Calcd for C₂₆H₃₈N₂O₃Sn: C, 57.3; H, 7.0; N, 5.1. For R = Ph·0.5Me₂C=O: red-orange blocks, yield 63%, mp 139–140 °C. Anal. Found: C, 63.4; H, 4.6; N, 4.4. Calcd for C_{33.5}H₂₉N₂O_{3.5}Sn: C, 63.4; H, 4.6; N, 4.4. For R = cHex: orange blocks, yield 68%, mp 144–145 °C. Anal. Found: C, 61.7; H, 7.0; N, 4.5. Calcd for C₃₂H₄₄N₂O₃Sn: C, 61.7; H, 7.1; N, 4.5. NMR data is given below.

Crystallography. Crystallographic data and refinement details are given in Table 1. Intensity data were collected at room temperature on a Rigaku AFC6R diffractometer using the ω -2 θ scan technique and graphite-monochromatized Mo K α radiation (λ 0.710 73 Å). The data sets were corrected routinely for Lorentz and polarization effects,¹⁴ and an empirical absorption correction¹⁵ was applied in each case. The structures were solved by direct methods,¹⁶ and each were refined by a full-matrix least-squares procedure based on *F*.¹⁴ Non-hydrogen atoms were refined with anisotropic displacement parameters, and hydrogen atoms were included in the models at their calculated positions (C–H 0.97 Å); the O–H atom was located in the analysis for R = Me and cHex. Disorder was noted in the structure of the R = ⁿBu compound associated with the C(41)–C(44) butyl group. These atoms

were refined isotropically and the methyl atom modeled over three sites of equal weight; no hydrogen atoms were included for this group. A σ weighting scheme was applied, i.e., $w = 1/\sigma^2(F)$, and the refinement was continued until convergence in each case. Neutral scattering factors employed were as included in teXsan,¹⁴ and diagrams for R = Me and cHex were drawn with ORTEP¹⁷ at the 50% probability level.

Basic NMR Characterization. ¹H and ¹³C NMR assignments have been achieved using standard 1D ¹H and ¹³C NMR and gradient-assisted 2D ¹H–¹³C HMQC and HMBC spectroscopy, as described earlier,¹⁸ performed on the R = Et compound, the data being then subsequently extrapolated to the other compounds owing to data similarity. All data were obtained from CDCl₃ solutions. Chemical shifts in ppm (TMS). Multiplicities and ⁿJ(¹H–¹H) coupling constants in hertz are given in parentheses. Abbreviations: s = singlet; d = doublet; dd = doublet of doublets; m = complex pattern; t = triplet. ⁿJ(¹H–^{119/117}Sn) and ⁿJ(¹³C–^{119/117}Sn) are given between square brackets. A single value is given when ⁿJ(¹³C– or ¹H–¹¹⁹Sn) and ⁿJ(¹³C– or ¹H–¹¹⁷Sn) are unresolved.

R'COOSnMe₃. ¹H NMR: H3 8.05 (d, 8); H4 7.46 (dd 8, 8); H5 7.55 (dd 8, 8); H6 7.87 (d, 8); H3' 6.91 (d, 8); H4' 7.13 (d, 8); H6' 7.73 (s); OH 12.78 (s); CH₃ 2.36 (s); Sn–CH₃ 0.67 [²J(¹H–^{119/117}Sn) = 57]. ¹³C NMR: C1 149.2; C2 128.4; C3 131.8; C4 130.2; C5 132.1; C6 116.6; C1' 137.9; C2' 150.8; C3' 119.4; C4' 134.6; C5' 128.8; C6' 133.3; CH₃ 20.3; Sn–CH₃ –1.9 [¹J(¹³C–^{119/117}Sn) = 392/375].

R'COOSnEt₃. ¹H NMR: H3 8.05 (d, 8); H4 7.46 (dd 8, 8); H5 7.56 (dd 8, 8); H6 7.86 (d, 8); H3' 6.91 (d, 8); H4' 7.13 (dd, 8, 2); H6' 7.73 (s); OH 12.71 (s); CH₃ 2.36 (s); Sn–CH₂ + CH₃ (Et) 1.03–1.63 (m). ¹³C NMR: C1 149.3; C2 130.2; C3 131.9; C4 130.2; C5 132.0; C6 115.9; C1' 138.0; C2' 150.8; C3' 118.5; C4' 134.5; C5' 128.7; C6' 133.3; CH₃ 20.3; Sn–CH₂ 8.4 [¹J(¹³C–^{119/117}Sn) = 363/347]; CH₃ (Et) 9.9 [²J(¹³C–^{119/117}Sn) = 25].

R'COOSnBu₃. ¹H NMR: H3 8.01 (d, 8); H4 7.47 (dd 8, 8); H5 7.53 (dd 8, 8); H6 7.83 (d, 8); H3' 6.89 (d, 8); H4' 7.11 (d, 8); H6' 7.72 (s); OH 12.67 (s); CH₃ 2.35 (s); Sn–CH₂ + CH₂(β) + CH₂(γ) 1.24–1.69 (m); CH₃ (Bu) 0.88 (t, 7). ¹³C NMR: C1 149.3; C2 130.4; C3 131.7; C4 130.1; C5 131.9; C6 115.9; C1' 138.0; C2' 150.7; C3' 118.5; C4' 134.5; C5' 128.6; C6' 133.3;

(14) teXsan: Structure Analysis Software; Molecular Structure Corporation: The Woodlands, TX, 1996.

(15) Walker, N.; Stuart, D. *Acta Crystallogr. Sect. A* **1983**, *39*, 158.

(16) Burla, M. C.; Camalli, M.; Cascarano, G.; Giacovazzo, C.; Polidori, G.; Spagna, R.; Viterbo, D. *J. Appl. Crystallogr.* **1989**, *22*, 389.

(17) Johnson, C. K. ORTEP. Report ORNL-5138, Oak Ridge National Laboratory, Oak Ridge, TN, 1976.

(18) Willem, R.; Bouhdid, A.; Kayser, F.; Delmotte, A.; Gielen, M.; Martins, J. C.; Biesemans, M.; Mahieu, B.; Tiekink, E. R. T. *Organometallics* **1996**, *15*, 1920.

CH₃ 20.3; Sn-CH₂ 17.0 [¹J(¹³C-^{119/117}Sn) = 353/336]; CH₂(β) 27.9 [²J(¹³C-^{119/117}Sn) = 20]; CH₂(γ) 27.1 [³J(¹³C-^{119/117}Sn) = 65]; CH₃ (Bu) 13.7.

R'COOSnPh₃. ¹H NMR: H3 8.19 (d, 8); H4 7.35–7.45 (m) overlapping with H_{m,p}; H5 7.58 (dd 8,8); H6 7.79–7.85 (m) overlapping with H_o; H3' 6.59 (d, 8); H4' 6.92 (d, 8); H6' 7.65 (s); OH 12.68 (s); CH₃ 2.35 (s); H_o 7.79–7.85 (m) overlapping with H6; H_{m,p} 7.35–7.45 (m) overlapping with H4. ¹³C NMR: C1 150.2; C2 130.3 overlapping with C_p; C3 132.7; C4 130.1; C5 133.0; C6 116.4; C1' 138.2; C2' 150.9; C3' 118.7; C4' 134.8; C5' 128.7; C6' 133.5; CH₃ 20.4; Sn-Ci 138.5 [¹J(¹³C-^{119/117}Sn) = 628/605]; C_o 137.3 [²J(¹³C-^{119/117}Sn) = 47]; C_m 129.1 [³J(¹³C-^{119/117}Sn) = 63]; C_p 130.3 overlapping with C2.

R'COOSn(cHex)₃. ¹H NMR: H3 8.01 (d, 8); H4 7.47 (dd 8, 8); H5 7.53 (dd 8, 8); H6 7.80 (d, 8); H3' 6.92 (d, 8); H4' 7.12 (d, 8); H6' 7.72 (s); OH 12.45 (s); CH₃ 2.35 (s); Sn-CH + CH₂(β) + CH₂(γ) + CH₂(δ) 1.31–1.97 (m). ¹³C NMR: C1 149.6; C2 130.6; C3 131.7; C4 130.1; C5 131.8; C6 116.1; C1' 138.0; C2' 150.7; C3' 118.5; C4' 134.4; C5' 128.5; C6' 133.3; CH₃ 20.3; Sn-CH 34.4 [¹J(¹³C-^{119/117}Sn) = 335/320]; CH₂(β) 31.2 [²J(¹³C-^{119/117}Sn) = 15]; CH₂(γ) 29.1 [³J(¹³C-^{119/117}Sn) = 67/64]; CH₂(δ) 27.0 [⁴J(¹³C-^{119/117}Sn) = 8].

Solid-State ¹¹⁷Sn NMR Measurements. All CP-MAS NMR spectra^{19,20} were recorded on a Bruker AC250 spectrometer, operating at 89.15 and 62.93 MHz for ¹¹⁷Sn and ¹³C nuclei, respectively, under the same experimental conditions as described previously.²¹ ¹¹⁷Sn chemical shift referencing is toward tetracyclohexyltin taken as a secondary reference at -97.35 ppm.

¹¹⁷Sn rather than the more common ¹¹⁹Sn spectra were recorded in order to overcome local radio interferences around 93.2 MHz.²² Comparing ¹¹⁷Sn and ¹¹⁹Sn NMR data is not a problem as primary ¹¹⁷Sn/¹¹⁹Sn isotopic effects are negligible.²³

The principal components of the ¹¹⁹Sn shielding tensors were analyzed according to Herzfeld and Berger²⁴ using WINFIT software.²⁵ They are reported, following Haeberlen's notation,²⁶ as the isotropic chemical shift ($\delta_{\text{iso}} = -\sigma_{\text{iso}}$), the anisotropy ($\zeta = \sigma_{33} - \sigma_{\text{iso}}$), and the asymmetry ($\eta = |\sigma_{22} - \sigma_{11}| / |\sigma_{33} - \sigma_{\text{iso}}|$), σ_{11} , σ_{22} , and σ_{33} being the three components of the shielding tensor expressed in its principal axis system with the following rule: $|\sigma_{33} - \sigma_{\text{iso}}| \geq |\sigma_{11} - \sigma_{\text{iso}}| \geq |\sigma_{22} - \sigma_{\text{iso}}|$. With this writing convention, ζ is a signed value expressed in ppm.

Solution-State ¹¹⁷Sn and ¹⁷O NMR Measurements. The samples were prepared by dissolving ca. 50 mg of compound in 500 μL of CDCl₃. The ¹¹⁷Sn NMR spectra were recorded at 303 K on a Bruker AC250 spectrometer, operating at 89.15 for ¹¹⁷Sn. ¹¹⁷Sn chemical shifts were referenced to $\Xi = 35.632$ 295 MHz.²⁷ ¹⁷O NMR spectra were recorded at natural abundance level on a sample containing ca. 200 mg/0.5 mL of C₆D₆, at 333 K, on a Bruker AMX500 spectrometer operating

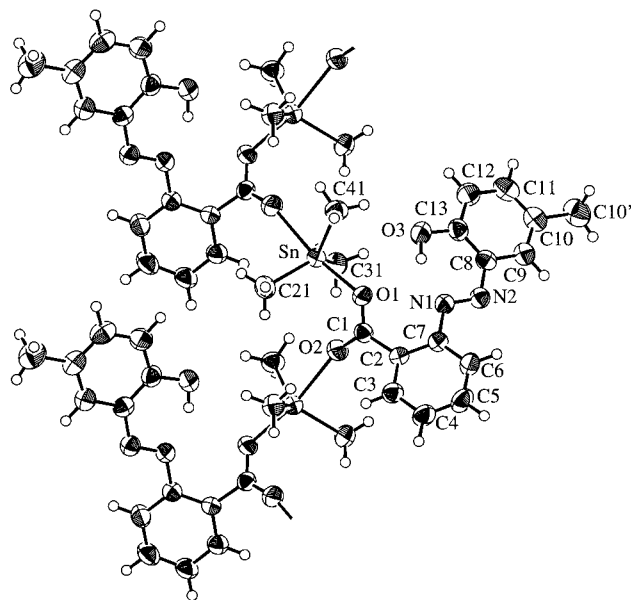


Figure 1. Crystallographic numbering scheme for [R₃Sn(O₂CR')]_n, R = Me (**1**); analogous structures and numbering schemes exist for R = Et (**2**) and R = ⁿBu (**3**).

at 67.8 MHz resonance frequency. The signals were referenced to external deionized water. Standard instrumental settings were used,²⁸ as explained elsewhere.²¹ The ¹⁷O chemical shift reproducibility is within 2 ppm.

Results and Discussion

Crystal Structures. The molecular structure of [Me₃Sn(O₂CR')] (**1**) is shown in Figure 1; the structures of R = Et (**2**) and R = ⁿBu (**3**) adopt the same motif as that for **1**, and selected interatomic parameters for the three structures are collected in Table 2. The structures of **1–3** adopt motif (II) and comprise distorted *trans*-R₃SnO₂ trigonal bipyramidal geometries. The tin atom lies 0.1735(3), 0.174(1), and 0.1980(4) Å out of their respective trigonal planes in the direction of the more tightly bound O(1) atoms. The carboxylate ligand is bidentate bridging; however, the Sn–O bonds thus formed are not equivalent. The disparity in the Sn–O bond distances, [O(1)–Sn–O(2)–Sn], increases in the order Me (0.323 Å) < Et (0.350 Å) < ⁿBu (0.415 Å). The lengths of the intramolecular Sn...O(2) separations, i.e., 3.175(4), 3.18(1), and 3.245(3) Å for **1–3**, respectively, are not consistent with significant bonding interactions. Intramolecular hydrogen-bonding interactions are noted in the structures. In **1**, O(3)–H...N(1) is 1.71 Å and O(3)–H...O(1) is 2.42 Å; the O–H atom was not located in the refinements of **2** and **3**.

A view of the unit cell contents for **1** is shown in Figure 2. The polymeric chain is propagated by the crystallographic 2₁ screw axis in the *b*-direction. The lattice can be described as being comprised of rows of tin atom coordination polyhedra, embedded between layers of carboxylate residues. These are, in turn, associated with neighboring layers via hydrophobic interactions. In the lattices of **2** and **3**, the polymer is propagated by 2₁ symmetry along the *c*- and *b*-axes, respectively, in a similar manner as that for **1**. The

(19) Bovey, F. A.; Jelinski, L.; Mirau, P. A. *Nuclear Magnetic Resonance Spectroscopy*, 2nd ed.; Academic Press Inc.: San Diego, CA, 1987; Chapter 8, pp 399–434.

(20) (a) Sebald, A. MAS and CP/MAS NMR of Less Common Spin-1/2 Nuclei. In *Solid State NMR II: Inorganic Matter*; Diehl, P., Fluck, E., Günther, H., Kosfeld, R., Seelig, J., Eds.; Springer-Verlag: Berlin, 1994; p 91. (b) Sebald, A. In *Physical Organometallic Chemistry. Advanced Applications of NMR to Organometallic Chemistry*; Gielen, M., Willem, R., Wrackmeyer, B., Eds.; John Wiley: Chichester, 1996; Chapter 5, pp 123–157.

(21) Biesemans, M.; Willem, R.; Damoun, S.; Geerlings, P.; Lahcini, M.; Jaumier, P.; Jousseau, B. *Organometallics* **1996**, *15*, 2237.

(22) (a) Koch, B. R.; Fazakerley, G. V.; Dijkstra, E. *Inorg. Chim. Acta* **1980**, *45*, L51. (b) Harrison, P. G. In *Chemistry of Tin*; Harrison, P. G., Ed.; Blackie & Son Limited: Glasgow, U.K., 1989; Chapter 3, p 113.

(23) McFarlane, H. C. E.; McFarlane, W.; Turner, C. J. *Mol. Phys.* **1979**, *37*, 1639.

(24) Herzfeld, J.; Berger, A. E. *J. Chem. Phys.* **1980**, *73*, 6021.

(25) Massiot, D.; Thiele, H.; Germanus, A. *Bruker Rep.* **1994**, *140*, 43.

(26) Haeberlen, U. *Adv. Magn. Reson. Suppl.* **1976**, *1*.

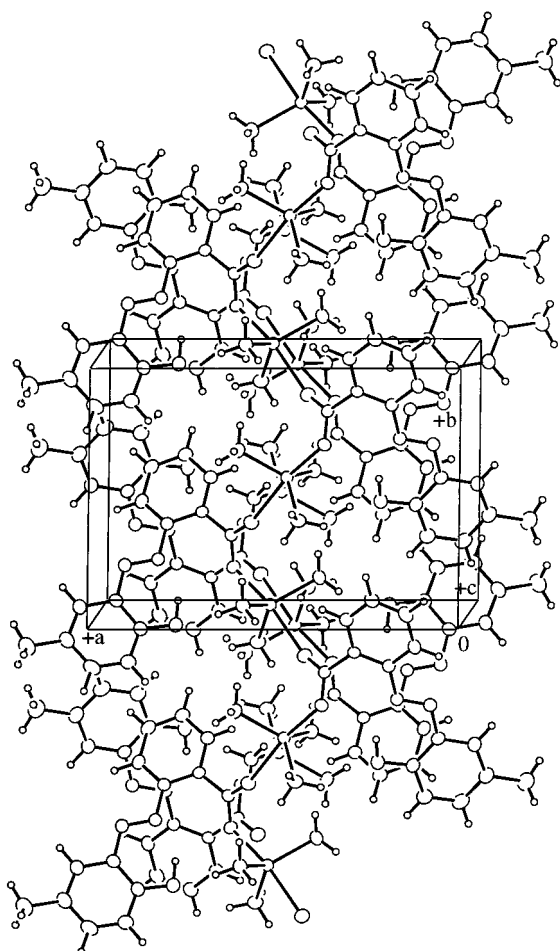
(27) (a) Davies, A. G.; Harrison, P. G.; Kennedy, J. D.; Puddephatt, R. J.; Mitchell, T. N.; McFarlane, W. *J. Chem. Soc. A* **1969**, 1136. (b) Mason, J. *Multinuclear NMR*; Plenum Press: New York, 1987; p 627.

(28) Boykin, D. W.; Chandrasekaran, S.; Baumstark, A. L. *Magn. Reson. Chem.* **1993**, *31*, 489.

Table 2. Selected Geometric Parameters (Å, deg) for $R_3Sn(O_2CR')$, $R = Me, Et, nBu, Ph,$ and $cHex$

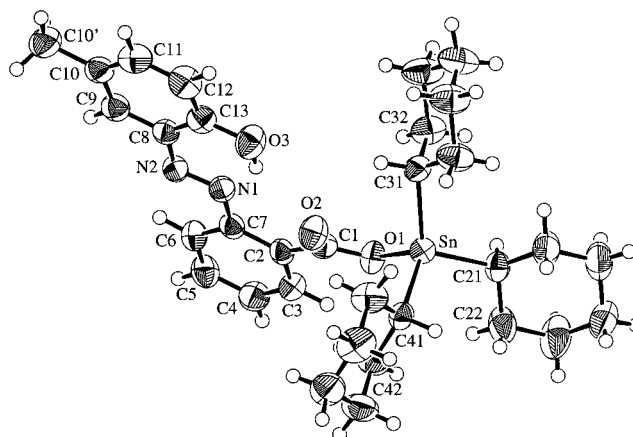
parameter	R = Me ^a	R = Et ^a	R = <i>n</i> Bu ^a	R = Ph ^{b,c}	R = cHex ^b
Sn–O(1)	2.164(3)	2.20(1)	2.164(3)	2.079(5)	2.076(3)
Sn–O(2)	2.487(3)	2.55(1)	2.579(4)	2.656(5)	2.759(4)
Sn–C(21)	2.111(5)	2.15(2)	2.139(6)	2.133(7)	2.161(5)
Sn–C(31)	2.111(5)	2.07(2)	2.125(5)	2.119(7)	2.150(6)
Sn–C(41)	2.104(5)	2.12(3)	2.151(6)	2.110(7)	2.151(4)
O(1)–C(1)	1.273(5)	1.29(2)	1.273(5)	1.297(8)	1.299(7)
O(2)–C(1)	1.226(5)	1.29(2)	1.233(5)	1.228(8)	1.228(7)
N(1)–N(2)	1.271(5)	1.23(2)	1.267(5)	1.273(7)	1.262(6)
O(1)–Sn–O(2)	170.6(1)	172.1(4)	173.8(1)	53.6(2)	51.7(1)
O(1)–Sn–C(21)	100.3(2)	96.3(2)	98.3(2)	95.3(2)	96.7(2)
O(1)–Sn–C(31)	94.1(2)	97.0(5)	89.9(2)	109.9(2)	107.2(2)
O(1)–Sn–C(41)	89.7(2)	90.5(7)	97.5(2)	113.3(2)	106.1(2)
O(2)–Sn–C(21)	88.3(2)	87.1(5)	84.1(2)	148.5(2)	148.1(1)
O(2)–Sn–C(31)	84.4(2)	86.9(5)	83.9(2)	86.7(2)	78.8(2)
O(2)–Sn–C(41)	83.2(2)	81.6(7)	85.9(2)	84.2(2)	84.9(2)
C(21)–Sn–C(31)	122.5(2)	124.2(7)	113.4(3)	111.9(3)	112.3(2)
C(21)–Sn–C(41)	114.6(2)	110.6(9)	122.4(2)	107.4(3)	111.5(2)
C(31)–Sn–C(41)	120.9(2)	123.2(9)	121.6(2)	116.9(3)	120.1(2)
Sn–O(1)–C(1)	120.7(3)	121(1)	123.6(3)	105.3(5)	109.3(3)
Sn–O(2)–C(1)	159.1(3)	144(1)	158.5(3)	80.0(4)	78.6(3)
O(1)–C(1)–O(2)	123.6(4)	120(1)	123.5(5)	121.0(7)	120.5(5)

^a Intermolecular O(2). ^b Intramolecular O(2). ^c Reference 13a, as Me₂C=O hemisolvate.

**Figure 2.** Unit cell contents for $[Me_3Sn(O_2CR')]_n$ (**1**).

polymeric structures found for **1–3** are not repeated in the structures of **(4)·0.5Me₂C=O**^{13a} and **(5)**.

The molecular geometry for **5** is illustrated in Figure 3, and selected interatomic parameters are listed in Table 2. The structure of **4** has been reported previously in the unsolvated form^{13b} and as an acetone hemisolvate,^{13a} derived parameters for the latter determination are also given in Table 2 (a consistent numbering

**Figure 3.** Crystallographic numbering scheme for $[cHex_3Sn(O_2CR')]$ (**5**).

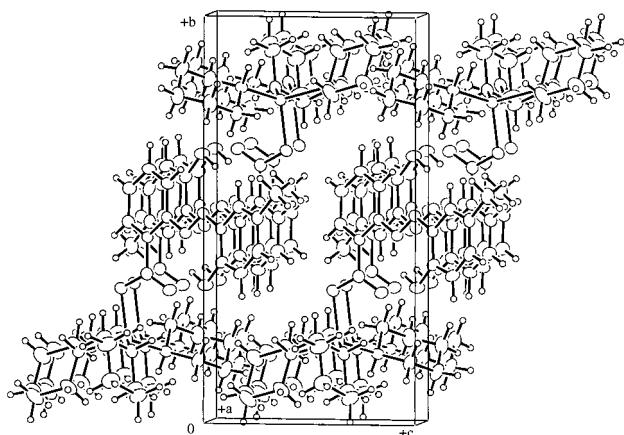
scheme was employed). The coordination geometry about the tin atom in **5** is best described as distorted C₃O tetrahedral, i.e., motif **1a**, with the range of angles subtended at tin being 96.7(2)–120.1(2)°. The Sn···O(2) separation of 2.759(4) Å is not considered a significant bonding interaction. The Pauling bond order²⁹ for Sn–O(1) and Sn–O(2) are calculated at 0.95 and 0.03, respectively. If the Sn···O(2) interaction is to be considered as a significant bonding interaction, then the geometry about the tin atom would be described as cis-R₃SnO₂ trigonal bipyramidal with the O(1), C(31), and C(41) atoms defining the trigonal plane. In this description, the Sn atom would lie 0.645(3) Å out of the equatorial plane in the direction of the C(21) atom. The major stereochemical role of the O(2) atom is to distort the tetrahedral geometry by opening up the C(21)–Sn–C(31) angle to 120.1(2)°. As for the structures described above, there is intramolecular hydrogen bonding with O(3)–H···N(1) 1.72 Å and O(3)–H···O(2) 2.19 Å. There are no intermolecular contacts <4.2 Å involving the tin atom. The structure of **4·0.5Me₂C=O** has been reported previously and is thus available for comparison.^{13a} The

(29) Pauling, L. *The Nature of the Chemical Bond*, 3rd ed.; Cornell University Press: Ithaca, NY, 1960.

Table 3. Solution and Solid State Data for Compounds 1–5^a

comps	IS ^b	QS ^c	$\delta^{117}\text{Sn}$		$\Delta\delta^{117}\text{Sn}^f$	$\delta^{17}\text{O}^g$	$^1J(^{13}\text{C}-^{119/117}\text{Sn})^h$
			solid ^d	solution ^e			
1 (R = Me)	1.37	3.76	24.7	148.1	123.4	275.6	392/375
2 (R = Et)	1.49	3.74	17.0	120.0	103.0	272.4	363/347
3 (R = ⁿ Bu)	1.50	3.85	23.3	123.0	99.7	273.8	353/336
4 (R = Ph)	1.23	2.45	-106.3	-105.9	0.4	279.8	628/605
5 (R = cHex)	1.50	2.76	-8.5	23.7	32.2	269.8	335/320

^a Solution data in CDCl₃ at 303 K, excepted when indicated otherwise. ^b Mössbauer ¹¹⁹Sn isomeric shift in mm/s. ^c Mössbauer ¹¹⁹Sn quadrupole splitting in mm/s. ^d Isotropic solid-state $\delta^{117}\text{Sn}$ chemical shifts in ppm, as measured with respect to (cHex)₄Sn taken as a secondary reference at -97.35 ppm. ^e Solution $\delta^{117}\text{Sn}$ chemical shifts in ppm, as measured with respect to $\Xi = 35.632\,295$ MHz. ^f $\Delta\delta^{117}\text{Sn} = \delta^{117}\text{Sn}(\text{solution}) - \delta^{117}\text{Sn}(\text{solid})$. ^g Reference: deionized water. ^h Measured in ¹³C spectra. ¹ $J(^{13}\text{C}-^{119/117}\text{Sn})$ not measurable in ¹³C solid-state spectra.

**Figure 4.** Unit cell contents for [cHex₃Sn(O₂CR')] (**5**).

substitution of cHex for Ph leads to a reduction in the Sn···O(2) distance, consistent with the increased Lewis acidity of the tin atom in the Ph₃Sn entity. Interestingly, although the Sn···O(2) distance in **4**·0.5Me₂C=O is less than that found in **5**, the distortions from the regular tetrahedral geometry, as judged from the angles subtended at tin, is less, i.e., 95.3(2)° to 116.9(3)°. The structure of **4**, as a substituted triphenyltin benzoate, exhibits the same four-coordinate geometry in the crystalline state as the unsubstituted parent triphenyltin benzoate.³⁰ This contrasts with the perfluorophenyl analogue of the latter which is of type **II**, as are most of the other triphenyl- and tri-*n*-butyltin carboxylates bearing a phenyl or perfluorophenyl moiety.^{30,31} It thus appears that, in the triphenyltin benzoate motif, the tin atom exhibits a very low Lewis acidity, since even in the solid state it is unable to extend significantly its coordination sphere. Not only do the molecular structures differ between **1–3** and **4**·0.5Me₂C=O – (**5**) but their crystal structures are also different.

A view of the crystal lattice of **5** is shown in Figure 4. Rows of centrosymmetrically related molecules of **5** run parallel to the *a*-axis; there is no evidence for extensive π - π interactions between the aromatic rings of the carboxylate residues. Adjacent rows align along the *c*-direction and are separated by hydrophobic contacts. Above and below the layers of carboxylate ligands are the cHex₃Sn entities which effectively sandwich the rows and associate with translationally related (along *b*) sandwiches via hydrophobic interactions between the

cHex groups. Similarly, in **4**·0.5Me₂C=O,^{13a} layers comprised of carboxylate residues in the *bc*-plane are sandwiched between layers of Ph₃Sn groups. Thus, whereas the structures of **1–3** are described as being comprised of rows of tin atom polyhedra sandwiched between carboxylate residues, the reverse is true for **4**·0.5Me₂C=O and **5** which are best described as being layers of carboxylate residues sandwiched between tin atom polyhedra.

Given the availability of the X-ray structures in the homogeneous series of compounds **1–5**, we investigated to which extent Sn–O distance parameters associated with the carboxylate ligand bonding are correlated with the Sn–O–Sn angle. Because the phenyl group exhibits a different electronic nature as compared to the alkyl groups, we analyzed correlations both including and excluding **4** with the triphenyltin moiety. The Sn–O(1) distance of the strong oxygen–tin bond shows a fair positive linear correlation with the O–Sn–O angle (Table 2): Sn–O(1) = +2.034 + 0.0008(2) \angle Sn–O–Sn, correlation coefficient $R = 0.965$ when the phenyl group is included; Sn–O(1) = +2.033 + 0.0008(3) \angle Sn–O–Sn, correlation coefficient $R = 0.946$ when the phenyl group is excluded. In contrast, the Sn–O(2) distance of the weak carbonyl oxygen–tin bond shows a much poorer, negative linear correlation with the Sn–O–Sn angle: Sn–O(2) = +2.781 – 0.0014(1) \angle Sn–O–Sn, correlation coefficient $R = 0.880$, when the phenyl group is included; this correlation improves when phenyl is omitted, Sn–O(2) = +2.852 – 0.0018(1) \angle Sn–O–Sn, $R = 0.937$. This appears to reflect fairly well electronic bonding characteristics of both Sn–O bonds, as a function of the nature of the organic substituent on tin, especially for nonaromatic triorganotin moieties.

Mössbauer Data. Mössbauer data are presented in Table 3. The values found for the quadrupole splitting (QS) may be divided into two sets. Compounds **1**, **2**, and **3**, with QS values of 3.76, 3.74, and 3.85 mm s⁻¹, respectively, conform perfectly well with a type **II** geometry, characterized by QS values ranging from 3.0 to 4.1 mm s⁻¹.^{30,32–35} Neglecting the minor but additional contributions from inorganic ligands to the quadrupole splitting, a value of 3.39 mm s⁻¹ arises from pqs (partial quadrupole splitting)³⁶ calculations. Compounds **4** and **5**, with QS values of 2.45 and 2.78 mm

(32) Molloy, K. C.; Blunden, S. J.; Hill, R. *J. Chem. Soc., Dalton Trans.* **1988**, 1259.

(33) Molloy, K. C.; Quill, K.; Blunden, S. J.; Hill, R. *Polyhedron* **1986**, 5, 959.

(34) Holmes, R. R.; Day, R. O.; Chandrasekhar, V.; Holmes, J. M. *Inorg. Chem.* **1986**, 25, 2490.

(35) Holmes, R. R.; Smith, P. J.; Day, R. O.; Chandrasekhar, V.; Holmes, J. M. *Inorg. Chem.* **1986**, 25, 2495.

(30) Willem, R.; Bouhdid, A.; Mahieu, B.; Ghys, L.; Biesemans, M.; Tiekink, E. R. T.; de Vos, D.; Gielen, M. *J. Organomet. Chem.* **1997**, 531, 151.

(31) Willem, R.; Bouhdid, A.; Biesemans, M.; Martins, J. C.; de Vos, D.; Tiekink, E. R. T.; Gielen, M. *J. Organomet. Chem.* **1996**, 514, 203.

Table 4. Solid-State ^{117}Sn NMR Data for Compounds 1–5^a

compds	δ_{iso}^b	ζ^c	η^d	σ_{11}^e	σ_{22}^e	σ_{33}^e
1 (R = Me)	24.7	229	0.00	-90	-90	254
2 (R = Et)	17.0	206	0.30	-117	-55	223
3 (R = ⁿ Bu)	23.3	190	0.30	-100	-43	214
4 (R = Ph)	-106.3	98	0.90	-200	-111	-8
5 (R = cHex)	-8.5	110	1.00	-119	-9	-102

^a Isotropic solid-state $\delta^{117}\text{Sn}$ chemical shifts in ppm, as measured with respect to (cHex)₄Sn taken as a secondary reference at -97.35 ppm. ^b $\delta_{\text{iso}} = -\sigma_{\text{iso}} = -(\sigma_{11} + \sigma_{22} + \sigma_{33})/3$ (ppm). ^c The anisotropy parameter $\zeta = \sigma_{33} - \sigma_{\text{iso}}$ (ppm). ^d The asymmetry parameter $\eta = |\sigma_{22} - \sigma_{11}|/|\sigma_{33} - \sigma_{\text{iso}}| = |\sigma_{11} - \sigma_{22}|/\zeta$. ^e σ_{11} , σ_{22} , and σ_{33} represent the three components of the shielding tensor expressed in its principal axis system with the following rule: $|\sigma_{33} - \sigma_{\text{iso}}| \geq |\sigma_{11} - \sigma_{\text{iso}}| \geq |\sigma_{22} - \sigma_{\text{iso}}|$.

s^{-1} , match quite well in the range of 2.3–3.0 mm s^{-1} characteristic for type **I** geometry, whether **Ia** or **Ib**.^{30,32–35} Partial quadrupole splitting calculations based on the contribution of the organic ligands give 2.52 and 2.74 mm s^{-1} , respectively, in excellent agreement with experimental values. Thus, the value of QS is confirmed to be a reliable solid-state structure indicator, at least to distinguish between the trans-R₃SnO₂ geometry of type **II** and the cis **I**.^{30–35} However, geometric effects on the electric field gradient are so dominant that they preclude any observation of side effects, such as the contribution of inorganic ligands. Within the aliphatic isostructural series **1–3**, no significant correlation was found between Mössbauer parameters and interatomic Sn–O distances.

Our data can, interestingly, be compared with literature data. For *trans*-(*m*-CH₃-C₆H₄)-CH=CH-COO-SnR₃ compounds,³⁷ similar values are found for R = Me, ⁿBu, and cHex (respectively, 3.55, 3.50, and 2.63 mm s^{-1} , as compared to the corresponding values for **1**, **3**, and **5** of 3.76, 3.85, and 2.76 mm s^{-1}), reflecting the same geometries as for our corresponding compounds **1**, **3**, and **5**; by contrast, for R = Ph, the literature³⁷ value of 3.41 mm s^{-1} reflects the polymeric geometry of type **II**, as opposed to that of **4** which is of type **I**. For complexes of the type Ph₃SnCl·L,³⁸ where L = X-C₆H₄-N=N-(*p*-CHO, *m*-OH)C₆H₄ (X = various substituents), the data are indicative of a cis geometry, as inferred by QS values of 2.45–2.52 mm s^{-1} .

Barbieri and Huber³⁹ report that isomeric shifts (IS) correlate to the electronegativity of metal-bonded atoms and groups, and, more correctly, to partial atomic charges on the metal atom in tin complexes. Table 3 indicates that the IS values reflect this correlation fairly well, being very similar for R = Et, ⁿBu, and cHex (respectively, 1.49, 1.50, and 1.50 mm s^{-1}), lowest for R = Ph (1.23), and intermediate for R = Me (1.37).

Solid-State ^{117}Sn NMR Data. Table 4 provides an overview of the solid-state ^{117}Sn NMR data. As expected, the isotropic ^{117}Sn chemical shifts of compounds **1–3**, as obtained from ^{117}Sn MAS spectra, around 20 ppm, properly reflect their five-coordination in the solid

state with tin chemical shifts of tri-*n*-butyltin compounds ranging from +40 to -60 ppm.^{30,31,40} By contrast, the value of -106.4 ppm for **4** is representative of four-coordination, since tin chemical shifts of five-coordinate triphenyltin carboxylates range from -180 to -280 ppm.^{30,31,40} Solution ^{119}Sn chemical shifts for aromatic tricyclohexyltin(IV) carboxylates are found in the range of 10–40 ppm and assigned to monomeric tetravalent species.⁴¹ The difference of 32 ppm to low frequency in the solid state with respect to the solution state observed for **5** is too small to be attributed to a coordination expansion, but probably reflects the constraints of the solid state. *trans*-(*m*-CH₃-C₆H₄)-CH=CH-COOSn(cHex)₃ is an example of tricyclohexyltin carboxylate³⁷ with no ^{119}Sn chemical shift difference between the solid and solution states.

CP-MAS ^{13}C NMR spectra did not provide useful information, the signal-to-noise ratio being too low for the observation of reliable $^1J(^{13}\text{C}-^{119/117}\text{Sn})$ coupling satellites.

The five-coordinate tin compounds **1–3** display axially symmetric shielding tensors and a shielding anisotropy ζ of the order of 200 ppm. This is in good agreement with the trans-R₃SnO₂ geometry around these tin atoms. Polymeric chains with tin in such a trans coordination environment are known for a variety of ligands X, e.g., X = hydroxide, carboxylate, and carbonate. Their ^{119}Sn CP-MAS spectra invariably show large shielding anisotropies with axial or close to axial symmetry, the most deshielded unique tensor component usually coinciding exactly or nearly with the O–Sn–O molecular axis.^{42,43} The tin sites in compounds **4** and **5** show asymmetric shielding tensors and narrower shielding patterns, both consistent with a strongly distorted tetrahedral environment.⁴⁴

Solution NMR. NMR data on the compounds **1–5** in CDCl₃ solution at room temperature are presented in Table 3. The ^{117}Sn NMR chemical shifts are neither temperature (233 K) nor concentration (factor 5 in dilution) dependent. The chemical shift data, as well as the $^1J(^{13}\text{C}-^{119/117}\text{Sn})$ coupling constants, are unambiguously characteristic for four-coordinate tin atoms.^{30,31,40,45–47} While the rather similar ^{117}Sn NMR chemical shifts for compounds **4** and **5** in solution and solid states indicate comparable four-coordination spheres for the tin atom, undoubtedly the five-coordinate polymeric structure of solid **1–3** is lost upon dissolution, four-coordinate monomeric structures being obtained. The latter behavior was observed previously for tri-*n*-butyltin as well as triphenyltin carboxylates.^{5,30,31} The ^{17}O NMR chemical shifts are in agreement with this assignment, their values being in the range observed

(40) Nadvornik, M.; Holeček, J.; Handlir, K.; Lyčka, A. *J. Organomet. Chem.* **1984**, 275, 43.

(41) Zhang, D.; Xie, Q.; Zheng, J.; Li, J. *Bopuxue Zazhi* **1990**, 7, 101; *Chem. Abstr.* **1990**, 113, 172227.

(42) Harris, R. K.; Packer, K. J.; Reams, P.; Sebald, A. *J. Magn. Reson.* **1987**, 72, 385.

(43) Komoroski, R. A.; Parker, R. G.; Mazany, A. M.; Early, T. A. *J. Magn. Reson.* **1987**, 73, 389.

(44) Kümmerlen, J.; Sebald, A.; Reuter, H. *J. Organomet. Chem.* **1992**, 427, 309.

(45) Holeček, J.; Nadvornik, M.; Handlir, K.; Lyčka, A. *J. Organomet. Chem.* **1983**, 241, 177.

(46) Holeček, J.; Handlir, K.; Nadvornik, M.; Lyčka, A. *J. Organomet. Chem.* **1983**, 258, 147.

(47) Lyčka, A.; Nadvornik, M.; Handlir, K.; Holeček, J. *Czech. Chem. Commun.* **1984**, 49, 1497.

(36) Parish, R. V. In *NMR, NQR, EPR and Mössbauer Spectroscopy in Inorganic Chemistry*; Burgess, J., Ed.; Ellis Horwood Series in Inorganic Chemistry; Ellis Horwood: London, 1990; pp 140–150.

(37) Danish, M.; Ali, S.; Mazhar, M.; Badshah, A.; Choudhary, M. I.; Alt, H. G.; Kehr, G. *Polyhedron* **1995**, 14, 3115.

(38) Sarma, K. K.; Basu Baul, T. S.; Rivarola, A.; Agrawal, R. P. *Polyhedron* **1994**, 13, 2217.

(39) Barbieri, R.; Huber, F. *Gazz. Chim. Ital.* **1993**, 123, 223.

previously by Lyčka and Holeček.⁴⁸ The ¹⁷O NMR chemical shifts lie in a range (~269–276 ppm) which approximately corresponds to the average of typical carbonyl (~360–370 ppm) and alkoxy (~160–170 ppm) oxygen values of organic esters such as butyl acetate.^{19,49,50} Thus, the ¹⁷O NMR chemical shifts are characteristic for a fluxional carboxylate in which the tin atom “jumps” from one carboxylate oxygen to the other within a rapid ¹⁷O NMR time scale.⁴⁸ An alternative, NMR indistinguishable formulation is that the carboxylate π -electrons are delocalized, resulting in a local structure of *C_s* symmetry at tin, where the three organic moieties, together with the tin atom, form a trigonal pyramid, the two carboxylate oxygens binding at the opposite side of the tin atom, with ¹/₂ bond order for each Sn–O bond.

Correlations between NMR Parameters and Sn–O Bond Distances. The availability of the X-ray structures as well as of the solid- and solution-state ¹¹⁷Sn NMR chemical shifts for **1–5** prompted an examination of how ¹¹⁷Sn NMR chemical shifts may be correlated with the Sn–O bond distance parameters. No useful correlation of any type could be found between ¹¹⁷Sn NMR chemical shifts, in solid or solution states, and the Sn–O(1) bond distances. The same holds for Sn–O(2), except when the R = Ph compound is omitted, in which case fair linear correlations are obtained for $\delta(^{117}\text{Sn})_{\text{solid}}$ and $\delta(^{117}\text{Sn})_{\text{solution}}$, respectively, $\delta(^{117}\text{Sn})_{\text{solid}} = -340(77) - 126(30) d(\text{Sn}-\text{O}(2))$, $R = 0.947$ and $\delta(^{117}\text{Sn})_{\text{solution}} = 1314(130) - 466(50) d(\text{Sn}-\text{O}(2))$, $R = 0.988$. As both Sn–O bonds were expected to modulate chemical shift data, we assessed correlations between $\delta(^{117}\text{Sn})_{\text{solid}}$ or $\delta(^{117}\text{Sn})_{\text{solution}}$ and $\Delta d(\text{Sn}-\text{O})$, where $\Delta d(\text{Sn}-\text{O}) = d(\text{Sn}-\text{O}(2)) - d(\text{Sn}-\text{O}(1))$. Results remain fair (but do not improve), $\delta(^{117}\text{Sn})_{\text{solid}} = 54(11) - 90(23) \Delta d(\text{Sn}-\text{O})$, $R = 0.939$ and $\delta(^{117}\text{Sn})_{\text{solution}} = 251(24) - 332(50) \Delta d(\text{Sn}-\text{O})$, $R = 0.978$, again only when compound **4** is omitted.

To find a correlation reflecting as much as possible only Sn–O distances, it was anticipated that the difference in chemical shifts between solid and solution states, $\Delta\delta(^{117}\text{Sn}) = \delta(^{117}\text{Sn})_{\text{solution}} - \delta(^{117}\text{Sn})_{\text{solid}}$ might reflect more properly the electronic properties of the carboxylate binding only, more specifically the Sn–O(2) bond, as the latter is obviously cleaved in solution; the underlying assumption is that the organic groups contribute in comparable amounts to the chemical shift values in solution and solid states, so that the difference of chemical shifts $\Delta\delta(^{117}\text{Sn})$ would cancel out these organic group contributions. Good correlations were obtained, mainly with $d(\text{Sn}-\text{O}(2))$ but also with $\Delta d(\text{Sn}-\text{O})$, again only when the R = Ph compound is omitted: $\Delta\delta(^{117}\text{Sn}) = 972(51) - 340(20) d(\text{Sn}-\text{O}(2))$, $R = 0.997$ and $\Delta\delta(^{117}\text{Sn}) = 197(14) - 242(30) \Delta d(\text{Sn}-\text{O})$, $R = 0.984$, respectively; these correlation coefficients drop to 0.91 or even lower when **4** is included.

These results indicate that $\Delta\delta(^{117}\text{Sn})$ rather than $\delta(^{117}\text{Sn})_{\text{solution}}$ or $\delta(^{117}\text{Sn})_{\text{solid}}$ alone is a good indicator of the increase in coordination number in the solid state, but only within the aliphatic series. This holds whenever the latter extension is reflected by the Sn–O(2)

distance itself or by its difference with respect to the Sn–O(1) distance. Thus, the tin-bound phenyl group displays a singular behavior. The deviation from the correlation is clearly induced by the mesomeric effect of the phenyl group and not by a different geometry as compound **5**, with its different geometry and the steric effect of the tricyclohexyltin moiety as compared to **1–3**, fitting the correlation well. As shown below, the deviation is caused by a “nonmatching” Sn–O(2) distance of **4** rather than ¹¹⁷Sn NMR chemical shift difference between solution and solid states. Clearly, the mesomeric effects do not express their influence to the same extent in the solid and solution states, unlike the inductive effects, as evidenced by the fact that using $\Delta\delta(^{117}\text{Sn})$ in order to cancel out the effect of the organic group does not improve the correlation coefficients when the R = Ph compound is included. Such correlations are of course only meaningful when the solvent has no coordinating properties, as is the case here. The absence of a correlation with $d(\text{Sn}-\text{O}(1))$ suggests little influence of the aggregation state on the length of the Sn–O(1) bond or, at least, a cancellation effect similar to that of the organic groups being included in $\Delta\delta(^{117}\text{Sn})$.

Literature data mention that linear correlations exist between solution $\delta^{119}\text{Sn}$ values and QS, both parameters being essentially controlled by similar nucleus properties, namely, imbalances of electron distributions due to electronegativity differences between the ligands.^{51,52} Such correlations exist for **1–5**; however, it is noted that correlating QS with either $\delta^{117}\text{Sn}_{\text{solution}}$ or $\delta^{117}\text{Sn}_{\text{solid}}$ individually gives inferior results than correlating QS with $\Delta\delta^{117}\text{Sn}$: QS = 2.44(0.14) + 0.0121(0.0015) $\Delta\delta^{117}\text{Sn}$, $R = 0.976$. Omitting **4** decreases only the quality of the correlation coefficient: QS = 2.43(0.28) + 0.0121(0.0029) $\Delta\delta^{117}\text{Sn}$, $R = 0.948$. The latter findings confirm not only that the nature of the organic group on the tin atom contributes to similar extents to the values of $\delta^{117}\text{Sn}_{\text{solid}}$ and $\delta^{117}\text{Sn}_{\text{solution}}$ but that this now even holds for the phenyl group. This is consistent with a previous statement that π -electron effects are less important for QS,⁵² confirming essentially the Sn–O(2) distance to be affected by the mesomeric effect of the phenyl group rather than $\Delta\delta^{117}\text{Sn}$ or QS. This is further supported by the fact that the parallel behavior of QS and ¹¹⁷Sn NMR chemical shifts is geometry independent.

Relationship between Motifs I and II. Given that the solution NMR study has shown that all five species are monomeric in solution, the crystallization process for **1–5** must be inherently similar in that monomeric units must deposit out of solution or commence aggregation just prior to crystallization. A common feature of the five determined X-ray structures is the appearance of rows of tin atom polyhedra either connected as in **1–3** or not as is **4**·0.5Me₂C=O and **5** (see Figure 5). It is possible to envision, based on the experimental evidence obtained for this particular series of compounds, a scenario where monomeric units are deposited in layers, comprising rows of tin atoms, and in the case of small tin-bound organic substituents, aggregation, i.e., the expected maximization of intermolecular forces, occurs via Sn → O contacts, leading

(48) Lyčka, A.; Holeček, J. *J. Organomet. Chem.* **1985**, *294*, 179.

(49) Orsini, F.; Severini Ricca, G. *Org. Magn. Reson.* **1984**, *22*, 653.

(50) Exner, O.; Dahn, H.; Pěchy, P. *Magn. Reson. Chem.* **1992**, *30*, 381.

(51) Ahmet, M. T.; Houlton, A.; Frampton, C. S.; Miller, J. R.; Roberts, R. M. G.; Silver, J.; Yavari, B. *J. Chem. Soc., Dalton Trans.* **1992**, 3085.

(52) Parish, R. V.; Platt, R. H. *Chem. Commun.* **1968**, 1118.

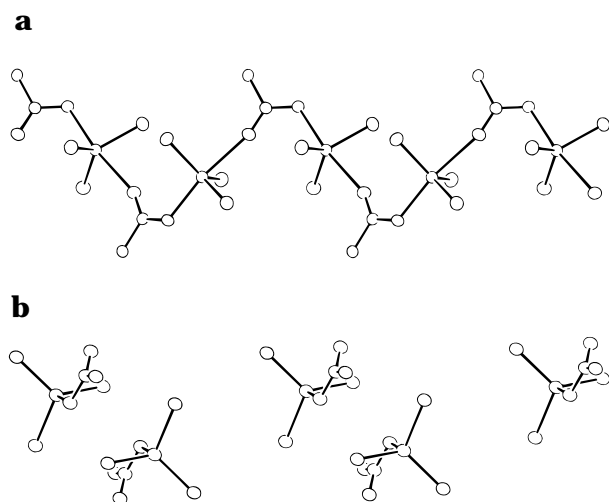


Figure 5. Arrangement of tin atoms in (a) motif **II** and (b) motif **Ia**; see the text.

to polymeric arrays. In the case where larger tin-bound substituents are present, such aggregation cannot occur owing to steric hindrance, and hence, mononuclear species are found in the solid state. Supporting evidence for this conclusion is found in the separation between the tin atoms in the respective crystal lattices.

It has been noted previously that the repeat distance in carboxylate-bridged triorganotin species **II** is 5.19 ± 0.21 Å, i.e., independent of tin-bound substituents and carboxylate residues.⁵³ In the three compounds in the present study that adopt this motif, the separations are 4.89, 5.20, and 5.03 Å for **1**, **2**, and **3**, respectively. As noted above, all five structures feature rows of tin atom

(53) Ng, S. W.; Wei, C.; Kumar Das, V. G. *J. Organomet. Chem.* **1988**, *345*, 59.

polyhedra, and thus, it is possible to determine the analogous "repeat" distances for $4 \cdot 0.5\text{Me}_2\text{C}=\text{O}$ and **5** as well. These are 4.75 and 5.17 Å, respectively. The polymeric motif could be adopted for each of $4 \cdot 0.5\text{Me}_2\text{C}=\text{O}$ and **5** (Figure 5b) if there was a rotation about the Sn–O(1) bond and a concomitant twisting of the R_3Sn entities leading to the structure illustrated in Figure 5a. It is proposed that this does not occur as the steric bulk of the Ph and cHex groups, as well as of the carboxylate residue, in **4** and **5** is too great to allow for the close approach of the molecules. Hence, it is concluded that, for the systems described herein, the adoption of motifs **Ia** or **II** in the solid state is driven, in the main, by steric considerations.

Acknowledgment. The Department of Science and Technology (India), for the award of a BOYSCAST Fellowship, the Department of Industry, Science and Technology (Australia), and North Eastern Hill University are thanked for enabling T.S.B.B. to work in Adelaide. The support of the crystallographic facility by the Australian Research Council and the financial support of the Belgian Flemish Science Foundation (FKFO, grants 2.0094.94, R.W., M.B. and S2/5 CD F198, M.G.), of the Belgian "Nationale Loterij" (grant 9.0006.93) (R.W., M.B.) and of the Fund for Scientific Research Flanders (Belgium, grant G.0192.98, R.W., M.B.) are gratefully acknowledged.

Supporting Information Available: Listings of crystal and refinement data, atomic coordinates and thermal parameters, all bond distances and angles for **1–3** and **5** in CIF format (26 pages). Ordering information is given on any current masthead page.

OM980504U